

## Reduced and quenched polarizabilities of interior atoms in molecules†

Cite this: *Chem. Sci.*, 2013, **4**, 2349

Aleksandr V. Marenich, Christopher J. Cramer\* and Donald G. Truhlar\*

Polarizability is a key molecular property controlling induction and dispersion forces in molecules, and atomic polarizabilities in molecules are widely used elements both in qualitative schemes for understanding molecular interactions and in quantitative methods for modeling them. Unfortunately, experimental probes of local polarizability are not readily available. Here we predict the polarizability of individual atoms and functional groups in a variety of systems, and we draw both general and specific conclusions with broad consequences. We find that the polarizability of the same functional group (e.g., the carbonyl group) can differ substantially, depending on the position of this group in a molecule (e.g., in a protein). More specifically, we find that the polarizability of buried atoms and groups is screened and thereby diminished; thus the outermost atoms and functional groups (for example, those lying closer to the molecular van der Waals surface) are more polarizable than buried ones, even when acted on by the same electric field. These findings mitigate against attributing isolated system behavior to molecular fragments since their polarizability depends on their environment, and the methods used here provide a way to probe molecular polarizability with a finer grain than has previously been possible.

Received 28th January 2013

Accepted 18th March 2013

DOI: 10.1039/c3sc50242b

[www.rsc.org/chemicalscience](http://www.rsc.org/chemicalscience)

### 1 Introduction

Polarizability plays a major role in both qualitative and quantitative considerations of reaction paths and molecular interactions. In the qualitative case, we note the role of polarizability in discussions of the softness and hardness of bases and acids, of frontier orbitals, and of perturbational molecular orbital analysis. In the quantitative case, we note that induction energies are directly proportional to polarizabilities, and polarizabilities play prominent roles in modeling dispersion interactions, substituent effects, and local solvation effects. As the progress of chemistry in many areas is closely tied to understanding and designing larger and more complex systems, it becomes more important to understand polarizability on a local basis. For example, the polarizability of that portion of a molecule or polymer that is close to a supramolecular interaction, an electronic excitation, or a charge transfer event is more relevant than the polarizability of the molecule or polymer as a whole. However, while molecular polarizabilities of many isolated atoms and molecules have been measured, practical experimental techniques are not available for

determining local polarizabilities of atoms or groups within molecules or polymers.

In the present article, we use density functional theory<sup>1</sup> to determine local polarizabilities in a variety of systems, including organic molecules, metal nanoparticles, and a polypeptide, and we draw general conclusions about the nature of local polarizability.

### 2 Theory

The concept of partitioning the electric polarizability of a molecule into atomic and interatomic contributions has been widely explored in the literature,<sup>2–19</sup> in particular with respect to the development of force field potentials and algorithms for computer-aided simulations.<sup>20</sup> The methods previously used for calculating distributed dipole and multipole polarizabilities include a partitioning of electronic properties over atomic centers using Bader's atoms-in-molecules topological theory<sup>21</sup> (as implemented, for instance, in ref. 4 and 7), Hirshfeld population analysis<sup>22,23</sup> (see ref. 16–18 for applications), or other partitioning techniques, for example, the site-specific partition scheme of Jackson *et al.*<sup>12</sup> using Voronoi polyhedra and the LoProp approach<sup>10</sup> utilizing Löwdin population analysis.<sup>24</sup> Other methods involve a determination of distributed polarizabilities by fitting them to reproduce the quantum-mechanically calculated induction (polarization) energy of a molecule polarized by a charge located at each point of a grid of charges around the molecule<sup>5</sup> and a computation of distributed polarizabilities by using a constrained density-fitting algorithm.<sup>11</sup>

Department of Chemistry, Chemical Theory Center, Supercomputing Institute, University of Minnesota, 207 Pleasant Street S.E., Minneapolis, MN, 55455-0431, USA. E-mail: [marenich@comp.chem.umn.edu](mailto:marenich@comp.chem.umn.edu); [cramer@umn.edu](mailto:cramer@umn.edu); [truhlar@umn.edu](mailto:truhlar@umn.edu)

† Electronic supplementary information (ESI) available: Cartesian coordinates for tested molecules, an example of a Gaussian input file for a calculation of distributed atomic polarizabilities using Hirshfeld population analysis, and additional details. See DOI: 10.1039/c3sc50242b

In the present study we analyze the polarizability in a variety of molecular systems using a simple method (similar to the one used earlier<sup>16</sup>) for partitioning the static dipole polarizability of an arbitrary molecule into atomic contributions by means of Hirshfeld population analysis<sup>22</sup> (as implemented, *e.g.*, in popular software packages<sup>25,26</sup>).

The  $\gamma\gamma$  component of the molecular static dipole polarizability tensor is calculated as

$$\alpha_{\gamma\gamma} = \left( \frac{\partial \mu_{\gamma}}{\partial F_{\gamma}} \right)_0 = \lim_{F_{\gamma} \rightarrow 0} \frac{\mu_{\gamma}(F_{\gamma}) - \mu_{\gamma}(0)}{F_{\gamma}} \quad (1)$$

where  $\mu_{\gamma}$  is the component of the dipole moment along axis  $\gamma$ , with  $\gamma = x, y$ , or  $z$ ,  $F_{\gamma}$  is the magnitude of a static electric field  $F$  along the  $\gamma$  axis, and “0” indicates  $F = 0$ . Averaging over  $\alpha_{xx}$ ,  $\alpha_{yy}$ , and  $\alpha_{zz}$  yields the spherically averaged molecular static dipole polarizability.

The quantity  $\alpha_{\gamma\gamma}$  can be partitioned over all atoms  $i$  in a molecule as

$$\alpha_{\gamma\gamma} = \sum_i \alpha_{\gamma\gamma i} \quad (2)$$

using the following relation:

$$\alpha_{\gamma\gamma i} = \lim_{F_{\gamma} \rightarrow 0} \frac{\mu_{\gamma i}(F_{\gamma}) - \mu_{\gamma i}(0)}{F_{\gamma}} \quad (3)$$

where the quantities  $\mu_{\gamma i}(F_{\gamma})$  and  $\mu_{\gamma i}(0)$  are the distributed contributions to the dipole moment, which are calculated by Hirshfeld population analysis, which is summarized for the convenience of the reader in Section 5 along with other computational details. The proposed algorithm has been tested against the topological partitioning of electronic properties (TPEP) method<sup>4,7</sup> based on Bader's atoms-in-molecules topological theory<sup>21</sup> on selected molecules as shown below.

Averaging over  $\alpha_{xxi}$ ,  $\alpha_{yyi}$ , and  $\alpha_{zxi}$  yields the spherically averaged static polarizability of atom  $i$ . The diagonal elements  $\alpha_{\gamma\gamma}$  of the *total* molecular dipole polarizability tensor must all be positive for a molecule in the ground electronic state because the dipole must increase in the direction of the field. However, negative values may occur for distributed polarizabilities,<sup>8</sup> even after spherical averaging, but the negative values are usually small. In the rest of this article we will discuss mostly spherically averaged static dipole polarizabilities (either total or distributed), and (as is conventional) we will simply call them polarizabilities.

### 3 Results and discussion

We first consider endohedral fullerenes. Table 1 shows distributed polarizabilities in the  $X@C_{60}$  molecules (where X is He, Ar, Mg, CO, CH<sub>4</sub>, or CF<sub>4</sub>) and partial charges on X and C<sub>60</sub> calculated using the CM5 charge model.<sup>27</sup> These results complement the results of previous calculations<sup>28,29</sup> on endohedral complexes of fullerenes that considered only noble gas atoms. Table 1 shows that the polarizability of the molecule X decreases substantially when X is incorporated inside the C<sub>60</sub> cage. The effect of the cage is most profound in the case of Mg. The atomic polarizability of Mg in  $Mg@C_{60}$  changes from 9.6 to

0.5 Å<sup>3</sup>, while the polarizability of the C<sub>60</sub> moiety increases by only 1.1 Å<sup>3</sup> in comparison with the polarizability of the free C<sub>60</sub> molecule. For nonmetallic guests, the distributed polarizability of C<sub>60</sub> in  $X@C_{60}$  remains almost the same as the polarizability of the free C<sub>60</sub> molecule.

The partial atomic charges in the last two columns of Table 1 show that there is no correlation between the magnitude of charge transfer from the enclosed atom to C<sub>60</sub> and the magnitude of the polarizability change for the enclosed atom or molecule. Thus, the change in polarizability is not due to the reduction in polarizability expected for a cation relative to its corresponding neutral, but rather is a shielding effect. The small value for the polarizability of the guest X in the  $X@C_{60}$  system can be understood by considering the C<sub>60</sub> molecule as a Faraday cage through which only a small portion of the external electric field can penetrate to the interior of C<sub>60</sub>,<sup>30</sup> leaving the ligand X essentially unpolarized. According to ref. 30, the applied field polarizes the C<sub>60</sub> cage, thereby inducing a dipole whose field in turn essentially cancels out the applied field inside the cage. Thus, the effect of the polarizable host (in this case the fullerene cage) on the guest (metal atom, rare gas atom, or organic molecule) is akin to placing the guest in a high-dielectric material that screens all electric interactions, not just the electrostatic ones but also the induced ones.

We find, however, that one does not require shielding by a bulk solvent or even a nanoparticle like C<sub>60</sub> to observe this effect. This is illustrated by the sulfur fluorides SF<sub>2</sub> and SF<sub>6</sub>, which are shown in Fig. 1. Table 2 shows that the polarizability of the exposed sulfur atom in SF<sub>2</sub> comprises 46% of the total molecular polarizability, whereas the polarizability contribution of the buried sulfur atom in SF<sub>6</sub> drops below 1% and is indeed a small negative number. Thus, the influence of four additional F atoms is effectively to extinguish the sulfur polarizability.

Next consider *meta*-nitroaniline (*m*-NA) and *para*-nitroaniline (*p*-NA); molecular structures of these systems are shown in Fig. 1. Table 3 presents distributed polarizabilities in the *m*-NA and *p*-NA molecules as computed with Hirshfeld population analysis in the present work (see Section 5 for computational details) compared to the same quantities computed in

**Table 1** Polarizabilities and distributed polarizabilities (in Å<sup>3</sup>) and partial charges (in a.u.) in the  $X@C_{60}$  complexes<sup>a</sup>

Molecule	Polarizability		Distributed polarizability		Partial charge	
	$X@C_{60}$	X	X	C <sub>60</sub>	X	C <sub>60</sub>
He@C <sub>60</sub>	78.5	0.1 (0.2)	0.1	78.4 (78.4)	0.03	-0.03
Ar@C <sub>60</sub>	78.7	0.3 (1.6)	0.3	78.4 (78.4)	0.13	-0.13
Mg@C <sub>60</sub>	80.0	0.5 (9.6)	0.5	79.5 (78.4)	0.13	-0.13
CO@C <sub>60</sub>	78.7	0.3 (1.7)	0.3	78.4 (78.4)	0.12	-0.12
CH <sub>4</sub> @C <sub>60</sub>	78.7	0.4 (2.0)	0.4	78.4 (78.4)	0.01	-0.01
CF <sub>4</sub> @C <sub>60</sub>	78.7	0.3 (2.4)	0.3	78.4 (78.4)	0.33	-0.33

<sup>a</sup> Numbers in parentheses are the polarizabilities of free species X and C<sub>60</sub> calculated at the same level of theory as used for the  $X@C_{60}$  systems. Calculations were performed using the M06-2X density functional and basis sets described in Section 5.

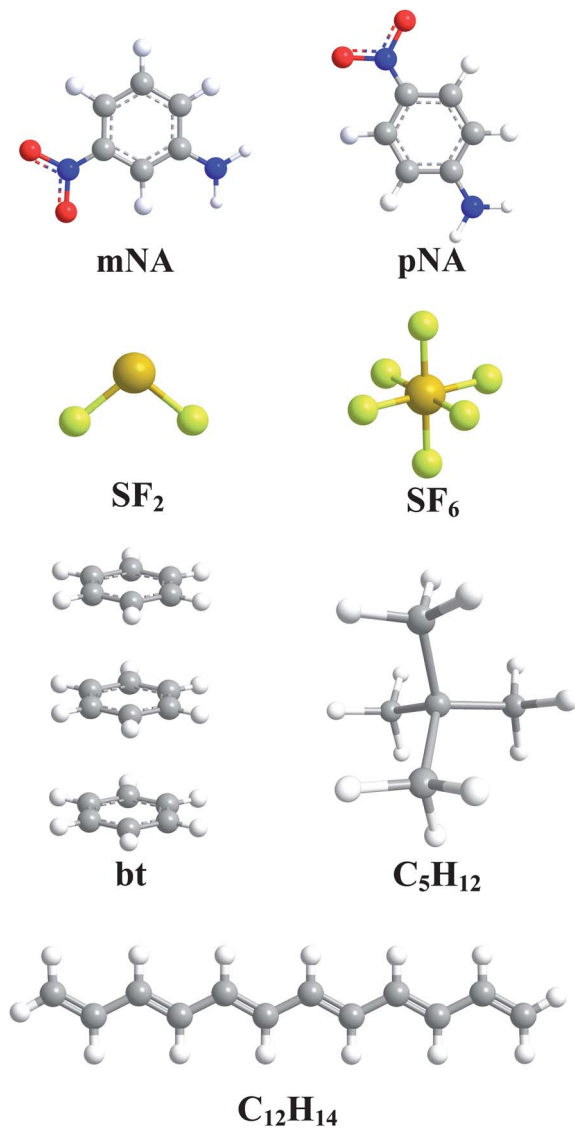


**Fig. 1** Molecular structures of *meta*-nitroaniline (*m*-NA), *para*-nitroaniline (*p*-NA), sulfur fluorides (SF<sub>2</sub> and SF<sub>6</sub>), benzene trimer (bt), neopentane (C<sub>5</sub>H<sub>12</sub>), and dodecahexaene (C<sub>12</sub>H<sub>14</sub>).

previous work<sup>9</sup> using the TPEP method<sup>4,7</sup> based on Bader's atoms-in-molecules topological theory.<sup>21</sup> The polarizability distribution method used in the present work agrees well with results obtained using a different approach at the same level of electronic structure theory. Both methods show that in these cases, where the functional groups are completely exposed in both molecules, the group polarizabilities of the nitro and amino groups are not extinguished and are similar in the two molecules. Furthermore, the polarizability of the benzene ring and its attached hydrogens is 6.8–7.4 Å<sup>3</sup>, which is smaller than the polarizability of isolated benzene, which is 9.8 Å<sup>3</sup> when calculated by the same method; this shows the effect of partial shielding by the two covalently bound ring substituents.

In contrast to the substituted but partially exposed benzene ring of the previous example, it is instructive to consider a stacked benzene trimer (shown in Fig. 1 where it is labeled bt),

**Table 2** Distributed polarizabilities (in Å<sup>3</sup>) in selected molecules<sup>a</sup>

Molecule	Fragment	Polarizability <sup>b</sup>
SF <sub>2</sub>	S	1.5
	Total (3 atoms)	3.2
SF <sub>6</sub>	S	−0.03
	Total (7 atoms)	4.0
bt	Central C <sub>6</sub> H <sub>6</sub>	8.0
	Total (36 atoms)	27.6
C <sub>5</sub> H <sub>12</sub>	Central C	0.04
	Total (17 atoms)	9.4
C <sub>12</sub> H <sub>14</sub>	20 interior atoms <sup>c</sup>	14
	Total (26 atoms)	36
C <sub>96</sub> H <sub>26</sub>	102 atoms <sup>d</sup>	163
	Total (122 atoms)	410
(CH <sub>3</sub> ) <sub>2</sub> CO · 12H <sub>2</sub> O	(CH <sub>3</sub> ) <sub>2</sub> CO	4.7 (5.9)
	Total (46 atoms)	21.8
Li <sub>91</sub> <sup>+</sup>	35 atoms <sup>e</sup>	−5.1
	Total (91 atoms)	904
1L2Y <sup>+</sup>	152 atoms <sup>f</sup>	38
	Total (304 atoms)	169

<sup>a</sup> Molecular structures are shown in Fig. 1–5. For each molecule the top line shows the sum of the polarizabilities of one or more “interior” atoms (as discussed in the text), and the second line gives the total polarizability. Calculations on Li<sub>91</sub><sup>+</sup> and 1L2Y<sup>+</sup> were performed using M06-L/6-31G(d) and HF/6-31G(d), respectively. Other calculations were performed using the M06-2X density functional and basis sets described in Section 5. <sup>b</sup> Number in parentheses is the polarizability of a free acetone molecule calculated at the same level of theory as for the cluster. <sup>c</sup> All atoms except the two terminal CH<sub>2</sub> groups. <sup>d</sup> All atoms except the ten CH groups selected in Fig. 4. <sup>e</sup> 35 atoms under the surface of Li<sub>91</sub><sup>+</sup>. <sup>f</sup> 152 innermost atoms relative to the center of nuclear charges in 1L2Y<sup>+</sup>.

**Table 3** Distributed polarizabilities (in Å<sup>3</sup>) in *m*-NA and *p*-NA

	<i>m</i> -NA			<i>p</i> -NA		
	M06-2X <sup>a</sup>	HF <sup>b</sup>	HF <sup>c</sup>	M06-2X <sup>a</sup>	HF <sup>b</sup>	HF <sup>c</sup>
−NH <sub>2</sub>	3.0	2.0	2.0	3.6	2.5	2.5
−C <sub>6</sub> H <sub>4</sub>	7.4	5.5	5.6	6.8	5.0	5.0
−NO <sub>2</sub>	3.6	2.5	2.5	4.1	2.8	2.9
Total	14.0	10.0	10.2	14.5	10.3	10.4

<sup>a</sup> Based on Hirshfeld population analysis at the M06-2X/MG3// M06-2X/MG3S level of theory. <sup>b</sup> Based on Hirshfeld population analysis at the HF/3-21G// M06-2X/MG3S level of theory. <sup>c</sup> See Table 2 in ref. 9; based on TPEP and HF/3-21G.

where the rings are unsubstituted and affected only by non-covalent interactions. The central benzene ring, which is shielded on both flat sides but not on the edges, has a polarizability of only 8.0 Å<sup>3</sup>, while the polarizabilities of the two outermost monomers are each 9.8 Å<sup>3</sup>. Therefore, the effective polarizability of the central benzene ring is ~18% smaller than the polarizability of an isolated benzene molecule. This effect is not an artefact resulting from averaging  $\alpha_{xxi}$ ,  $\alpha_{yyi}$ , and  $\alpha_{zzi}$  for each atom  $i$ . One can arrive at the same conclusion about the reduced polarizability of the central benzene ring in the trimer by treating the benzene monomers as anisotropic point dipoles in the electric field applied parallel (||) and perpendicular (⊥) to the stack axis  $z$ . In this case, we have  $\alpha_{||} = \alpha_{zz} = 4.8$

and  $\alpha_{\perp} = \alpha_{xx} = \alpha_{yy} = 9.5 \text{ \AA}^3$  for the central benzene ring in  $(\text{C}_6\text{H}_6)_3$  in comparison with  $\alpha_{\parallel} = 6.2$  and  $\alpha_{\perp} = 11.5 \text{ \AA}^3$  for an isolated  $\text{C}_6\text{H}_6$  molecule.

The two hydrocarbons, 2,2-dimethylpropane (*i.e.*, neopentane,  $\text{C}_5\text{H}_{12}$ ) and 1,3,5,7,9,11-dodecahexaene ( $\text{C}_{12}\text{H}_{14}$ ), both shown in Fig. 1 with distributed polarizabilities in Table 2, provide examples of shielding by covalently bound groups in nonpolar molecules. The polarizability of the centrally situated carbon atom in the neopentane molecule is nearly zero, and the total polarizability of  $\text{C}_5\text{H}_{12}$  is comprised almost entirely of the polarizabilities of the terminal methyl groups. As in the case of  $\text{X}@C_{60}$  and  $\text{SF}_6$ , the outermost fragments in the neopentane molecule (*i.e.*, the four  $\text{CH}_3$  groups) behave as a dielectric, thereby screening (reducing) the electrostatic interaction between the central atom or fragment and an external electric field. The polarizability of the dodecahexaene molecule is also distributed mainly to the outermost groups, in this case the two terminal  $\text{CH}_2$  groups, which constitute less than a quarter of the atoms but contribute 60% of the total polarizability. Even more dramatic is the graphene-like hydrocarbon with molecular formula  $\text{C}_{96}\text{H}_{26}$  as shown in Fig. 2. Table 2 shows that ten CH groups at two of the edges (highlighted in Fig. 2), although they constitute less than a sixth of the atoms, account for 60% of the polarizability.

An acetone–water cluster with twelve water molecules  $(\text{CH}_3)_2\text{CO} \cdot 12\text{H}_2\text{O}$  is shown in Fig. 3. The polarizability of the acetone molecule ( $4.7 \text{ \AA}^3$ ) inside this cluster drops by 20% in comparison with the total polarizability of the isolated  $(\text{CH}_3)_2\text{CO}$  molecule ( $5.9 \text{ \AA}^3$ ). The polarizability of the carbonyl group in the acetone solvated with twelve water molecules is only  $0.8 \text{ \AA}^3$ , as compared to the experimental polarizability<sup>31</sup> of  $1.95 \text{ \AA}^3$  for the isolated CO molecule. The polarizability of the acetone molecule inside clusters (not shown) with 24 and 36 water molecules reduces to  $4.3$  and  $4.0 \text{ \AA}^3$ , respectively.

We have already mentioned the analogy of the shielding effect to that of a dielectric medium. Since we are considering electronic polarizabilities at fixed geometries here, the relevant dielectric constant would be the one at optical frequencies, which equals the square of the optical refractive index  $n$ .

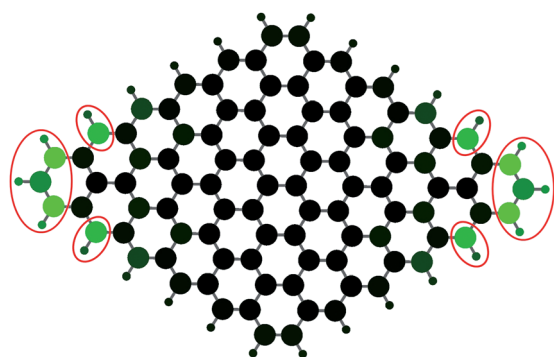


**Fig. 2** Molecular structure of  $\text{C}_{96}\text{H}_{26}$ . The color of the hydrogen and carbon atoms changes from dark green to light green with an increase in polarizability. Atomic contributions from the 20 selected atoms (out of 122) comprise 60% of the total molecular polarizability.

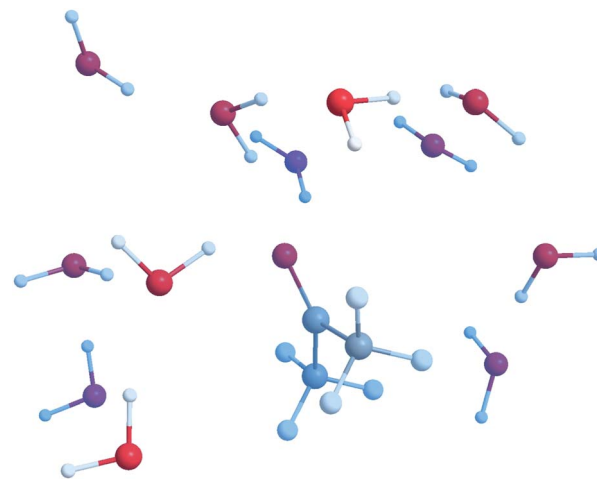


**Fig. 3** Molecular structure of the acetone–water cluster  $(\text{CH}_3)_2\text{CO} \cdot 12\text{H}_2\text{O}$ .

Since most materials have  $n^2$  in the range 1.8–6, this analogy would suggest a reduction of the polarizability for buried species by a factor of 1.8 to 6, or perhaps less since the molecular exterior occupies much less volume than that of a bulk dielectric medium. Nevertheless we saw that a much larger effect is possible in an endohedral fullerene. However, the effect can also be smaller; for example we saw that the polarizability of  $4.0 \text{ \AA}^3$  for acetone in the 36-water cluster is reduced by a factor of 1.5 from the isolated-molecule value of  $5.9 \text{ \AA}^3$ ; this is significant but less than  $n^2$  for bulk water, which is 1.8.

There is no experimental information available at this time for measuring the distributed polarizabilities predicted here. However, the dielectric-like screening of various molecules encapsulated in highly polarizable materials such as single-wall carbon nanotubes has been detected by observing the dramatically reduced IR vibrational intensities for endohedrally encapsulated molecules in comparison with the IR intensities for exohedrally bound molecules.<sup>32</sup>

Fig. 4 shows a large metallic nanoparticle, in particular a highly symmetric  $\text{Li}_{91}^+$  cluster. Table 2 shows that the 56 lithium atoms lying on the surface of the  $\text{Li}_{91}^+$  cube are responsible for all of the positive contributions to the total polarizability; the interior atoms make a small negative contribution.

The synthetic protein  $1\text{L}2\text{Y}^+$  (molecular formula  $\text{C}_{98}\text{H}_{150}\text{N}_{27}\text{O}_{29}$ ) from refs. 33 and 34 is shown in Fig. 5. The 152 outermost atoms (out of 304 atoms), as classified by their distance from the center of nuclear charge, contribute 77% of the total polarizability. A particularly interesting aspect of this case is that we found that the polarizability of the same functional group varies substantially depending on the position of the group in the molecule. As noted in ref. 19, many empirical force fields employ only 8–15 atom types for polarizabilities (sometimes using the same value for all non-hydrogen atoms). The present results show that the accuracy of such force fields and understanding based upon using them can be improved by using more specific atomic

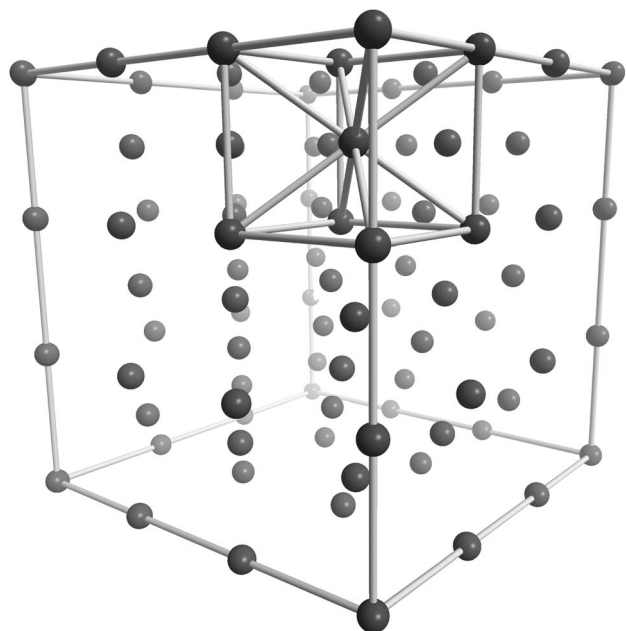


Fig. 4 Molecular structure of  $\text{Li}_9^+$ .

polarizabilities. For example, the polarizability varies from  $-0.4$  to  $4.0 \text{ \AA}^3$  over 21 carbonyl groups, while the corresponding CM5 partial charges<sup>27</sup> vary less dramatically (from  $-0.37$  to  $-0.46$  a.u. for the carbonyl O atom and from  $-0.03$  to  $-0.13$  a.u. for the whole CO group) and the CO distance remains roughly the same ( $\sim 1.23 \text{ \AA}$ ). The polarizability of the OH group varies from  $-0.3$  to  $2.1 \text{ \AA}^3$  over four occurrences, and the polarizability of the  $\text{COO}^-$  group is  $3.3$  and  $5.1 \text{ \AA}^3$  (a difference of a factor of more than 1.5) in two occurrences. Fig. 6 illustrates an example in which the polarizability ( $3.4 \text{ \AA}^3$ ) of a carbonyl group lying near the molecular perimeter is much larger than the polarizability ( $0.7 \text{ \AA}^3$ ) of a nearby carbonyl group situated in a less exposed portion of the

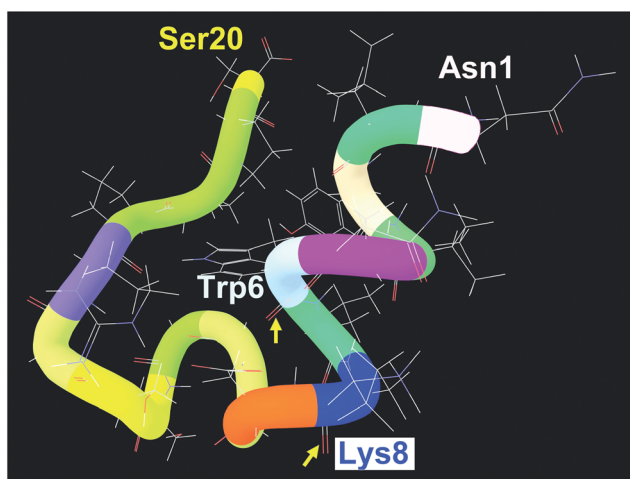


Fig. 5 Molecular structure of  $1\text{L}2\text{Y}^+$ . Color ribbons describe amino acid residues listed in full in the ESI.† The backbone carbonyl groups of residues 6 and 8 are shown in an expanded view in Fig. 6 and are singled out for discussion in the text.

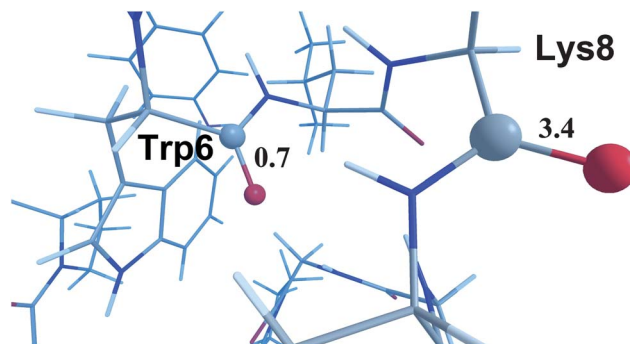


Fig. 6 Distributed polarizabilities of two CO groups (in  $\text{Å}^3$ ) in a fragment of the  $1\text{L}2\text{Y}^+$  molecule. The CO group on the right (which is part of the lysine-8 residue) lies near the molecular surface. The CO group on the left (which is part of the tryptophan-6 residue) lies near the center of nuclear charge. The positions of these groups in the  $1\text{L}2\text{Y}^+$  molecule are shown in Fig. 5.

polypeptide. The effects of various residues on substrate binding and enzyme catalysis are certainly affected by these polarizability variations.

It is worthwhile to mention that the various hyperpolarizabilities, which are important, for example, for nonlinear optics, may also be subject to this kind of shielding effect.

The present work is focused on studying gas-phase atoms, molecules and molecular clusters. Polarizability calculations for molecules in condensed phases have been considered elsewhere; see for example the work of Mennucci *et al.*<sup>35,36</sup> on static polarizabilities of several solutes in solution using the dielectric continuum approximation and mixed discrete-continuum solvation models. Both implicit solvent and explicit solvent molecules can substantially change the calculated polarizability of a solute molecule in comparison to that of an isolated molecule;<sup>35,36</sup> however, we expect that our conclusions about reduced polarizabilities of buried atoms and fragments derived from our gas-phase calculations will remain qualitatively valid in both gaseous and condensed phases. For example, according to the present calculations of the distributed polarizability of the previously studied  $(\text{CH}_3)_2\text{CO} \cdot 12\text{H}_2\text{O}$  cluster in water using the SMD solvation model,<sup>37</sup> the polarizability of the acetone molecule inside this cluster drops by 18% in comparison with the total polarizability of the unclustered acetone molecule in water, *i.e.*, by nearly the same margin as in the case of the corresponding gas-phase systems.

Although in the present article we do not investigate quantitatively the impact of polarizabilities on energetics, we note that induction energies are directly proportional to polarizabilities, and dispersion interactions can also be modeled in terms of polarizabilities, and the way that polarizabilities are evaluated can have a substantial impact on the magnitude of modeled induction and dispersion interactions, especially in van der Waals systems. We refer the reader to previous work on evaluating London dispersion interaction energies from distributed dipole and multipole atomic polarizabilities for some van der Waals dimers (see ref. 18 and references therein).

## 4 Conclusions

When a complex molecule is polarized it is important to know what part of the molecule is polarized and to what extent. We have partitioned polarizabilities over individual atoms and functional groups, and we have found that the polarizability of the same functional group (for example, CO or OH) can differ substantially, depending on the position of this group in a molecule, but a general trend does emerge. In particular, our calculations for a diverse set of molecules show that the polarizabilities of interior atoms and functional groups are greatly quenched, and the outermost atoms and functional groups in molecules are in general much more polarizable than their buried counterparts.

In several cases, the total molecular polarizability is comprised almost entirely of contributions from the outermost parts of the molecule, and the contributions from buried atoms can be safely neglected (they might even be negative). These findings can be important for future more reliable parameterizations of molecular mechanics force fields and electronic structure methods involving the embedding of molecular fragments in the electrostatic field and reaction field of their environment. More importantly though, they change our understanding of molecular interactions and environmental effects in qualitative ways.

We note that the reduced polarizability of buried atoms and groups in bulky molecules and clusters does not reflect a saturation of polarization associated with intramolecular interactions in the interior or a migration of the polarization to another part of the molecule, but rather derives from a Faraday-cage-like shielding of the interior by the electron density of the exterior of the system. The analogy to a Faraday cage is strong for C<sub>60</sub> but only qualitative for the other cases. We also note that the polarizability of a molecule being interior in a cluster with noncovalently bonded ligands (for example, the acetone molecule surrounded by several water molecules) is usually reduced but not quenched whereas the polarizability of a molecule (or an atom) inside a covalent molecular system (for example, CO at C<sub>60</sub> or the central carbon in neopentane) is quenched.

By its standard definition,<sup>31</sup> the electric dipole polarizability of an isolated molecule describes the dynamic response of the electron cloud to external electric fields. The distributed atomic polarizability of an atom in the molecule is calculated in the present study in terms of the response of the atom to a uniform electric field applied to the whole molecule. For interpretive or modeling purposes, polarizability can be redefined using the concept of local fields as introduced in ref. 3, *i.e.*, in terms of the response of one atom in the molecule to a local field at another atom, but here we use standard polarizabilities. Note that the diminished polarizability of interior atoms in response to a uniform electric field would be even further reduced if one considered the response of a molecule to a point charge, where the electric displacement due to the point charge would diminish as one moved farther away from the point charge and into the interior of the molecule with which it is interacting. The present paper is not about that geometry-dependent effect (which is elementary and well appreciated) but rather about the reduced polarizability response even to a uniform electric field.

## 5 Computational details

The  $\gamma$  component ( $\gamma = x, y,$  or  $z$ ) of the electric dipole moment of a molecule, which is invariant to choice of origin for an uncharged species, is expressed as follows (in atomic units)

$$\mu_\gamma = - \int r_\gamma \rho(\mathbf{r}) d^3\mathbf{r} + \sum_i Z_i R_{\gamma i} \quad (4)$$

where  $\rho(\mathbf{r})$  is the (positive) electron density at an arbitrary position  $\mathbf{r}$ , the index  $i$  runs over all atoms in the molecule,  $Z_i$  is the nuclear charge of atom  $i$ , and  $R_{\gamma i}$  is the  $\gamma$  component of the vector  $\mathbf{R}_i$  that defines the position of the nucleus of atom  $i$ . The density  $\rho(\mathbf{r})$  can be partitioned over all atoms in the molecule as

$$\rho(\mathbf{r}) = \sum_i \rho_i(\mathbf{r}) \quad (5)$$

where

$$\rho_i(\mathbf{r}) = w_i(\mathbf{r})\rho(\mathbf{r}) \quad (6)$$

The function  $w_i(\mathbf{r})$  in eqn (6) is a positive weight function defined for each atom in the molecule, and

$$\sum_i w_i(\mathbf{r}) = 1 \quad (7)$$

In the present work, the function  $w_i(\mathbf{r})$  is defined according to the Hirshfeld method.<sup>22</sup> The partitioned electron density on atom  $i$  can be expressed as

$$\rho_i(\mathbf{r}) = \rho_i^0(\mathbf{r}) + \delta\rho_i(\mathbf{r}) \quad (8)$$

where the first term on the right-hand side is the electron density of the isolated (neutral) atom  $i$ , and the second term is the deformation electron density of the atom in the molecule.<sup>22</sup> Therefore, eqn (4) can be rewritten as

$$\mu_\gamma = - \int r_\gamma \rho^0(\mathbf{r}) d^3\mathbf{r} + \sum_i Z_i R_{\gamma i} - \sum_i \int r_\gamma \delta\rho_i(\mathbf{r}) d^3\mathbf{r} \quad (9)$$

using

$$\rho^0(\mathbf{r}) = \sum_i \rho_i^0(\mathbf{r}) \quad (10)$$

The sum of the first and the second term in eqn (9) yields the dipole moment of a system of neutral atoms, which is zero. According to eqn (3) in ref. 22, we can introduce the partial charge on atom  $i$  as

$$q_i = - \int \delta\rho_i(\mathbf{r}) d^3\mathbf{r} \quad (11)$$

Using the nuclear coordinates  $R_{\gamma i}$  and partial atomic charges  $q_i$ , we can rewrite eqn (9) as

$$\mu_\gamma = \sum_i \mu_{\gamma i} \quad (12)$$

where

$$\mu_{\gamma i} = q_i R_{\gamma i} - \int (r_\gamma - R_{\gamma i}) \delta\rho_i(\mathbf{r}) d^3\mathbf{r} \quad (13)$$

This is the quantity needed for eqn (3) of this work.

All calculations were carried out with *Gaussian 09*.<sup>25</sup> The second term of eqn (13) is given by eqn (4) in ref. 22, and it can be recovered from a *Gaussian 09* output file with Hirshfeld charges computed using the keyword *pop = Hirshfeld*. See the ESI† for more detail.

The C<sub>60</sub> moiety in all X@C<sub>60</sub> systems has the geometry of free C<sub>60</sub> (I<sub>h</sub> symmetry). The geometries of C<sub>60</sub> and C<sub>96</sub>H<sub>26</sub> were optimized using PM6.<sup>38</sup> The geometry of the small protein 1L2Y<sup>+</sup> (molecular formula C<sub>98</sub>H<sub>150</sub>N<sub>27</sub>O<sub>29</sub>) was taken from ref. 33 and refined using the protein preparation wizard utility of the *Maestro* program.<sup>39</sup> The structure of Li<sub>91</sub><sup>+</sup> corresponds to the experimental body centered cubic structure of lithium crystals at ambient temperature and pressure (with a lattice parameter of 3.5 Å) given in ref. 40. The (CH<sub>3</sub>)<sub>2</sub>CO · 12H<sub>2</sub>O geometry is from ref. 41. The Cartesian coordinates for all other cases were optimized using the M06-2X (ref. 42 and 43)/MG3S (ref. 44) method. The Cartesian coordinates for all molecules are given in the ESI.†

Distributed atomic polarizabilities were calculated by numerical differentiation of analytical dipole moments by using the keyword *Field* in *Gaussian 09* and applying an electric dipole field of 0.001 a.u. in each direction (*x*, *y*, and *z*). We have found that the difference between the total polarizability calculated numerically and analytically is less than 0.5% in all studied cases. The polarizability calculations were performed using the density functionals M06-L (ref. 45) and M06-2X (ref. 42 and 43) and the Hartree-Fock (HF) method.<sup>46</sup> We used the following basis sets: MG3 (ref. 44 and 47) (which is identical to 6-311++G(2df,2p)<sup>46,48–50</sup> for first-row elements, H, and He), 6-31+G(d,p),<sup>46</sup> 6-31G(d),<sup>46</sup> and 3-21G.<sup>46</sup>

Calculations on *m*-NA and *p*-NA were carried out by the M06-2X/MG3 and HF/3-21G methods (the latter was used only for Table 3 for comparison with the results of earlier calculations<sup>9</sup>). Calculations on SF<sub>2</sub>, SF<sub>6</sub>, (C<sub>6</sub>H<sub>6</sub>)<sub>3</sub>, C<sub>5</sub>H<sub>12</sub>, C<sub>12</sub>H<sub>14</sub>, and (CH<sub>3</sub>)<sub>2</sub>CO · 12H<sub>2</sub>O were performed using M06-2X/MG3. Calculations on X@C<sub>60</sub> and C<sub>96</sub>H<sub>26</sub> were performed using the M06-2X density functional, the 6-31+G(d,p) basis set on H, C, O, and F, the MG3 basis on Mg and Ar, and the MG3 basis on He augmented with two additional diffuse *s* functions and two additional diffuse *p* functions; the exponential parameters of the added functions were obtained according to a procedure previously reported.<sup>51</sup> Calculations on Li<sub>91</sub><sup>+</sup> were performed by the M06-L/6-31G(d) method. Calculations on 1L2Y<sup>+</sup> were carried out using HF/6-31G(d).

Note that the spherically averaged distributed polarizabilities are invariant with regard to molecular rotations but not translations. We took the molecular center of nuclear charge as the origin of Cartesian coordinates. To confirm the validity of the conclusions made in this work, we have also performed calculations using translated coordinate systems for selected molecules. In the case of the X@C<sub>60</sub> molecules we have found that the polarizability distributed to the guest X retains the same small value (Table 1) if the coordinate system's origin moves to the C<sub>60</sub> wall. We have found that the polarizability of S in SF<sub>6</sub> remains the same upon moving the origin of the SF<sub>6</sub> coordinate system from S to one of the fluorine atoms. Moving the origin of the coordinate system of a molecule to an arbitrary position does not change the conclusion that the polarizability is distributed mainly to the outermost atoms and groups, for example, to the methyl groups in the case of neopentane. When we move the origin of the C<sub>12</sub>H<sub>14</sub> coordinate system from the center of nuclear charges to the

carbon atom of one of the CH<sub>2</sub> groups, the aggregated polarizability of the two CH<sub>2</sub> groups retains the same value but the individual polarizability of the CH<sub>2</sub> group at the origin is essentially redistributed towards another (outermost) CH<sub>2</sub> group.

The dipole moment ( $\mu$ ) of an isolated CO molecule derived from CM5 charges computed at the M06-2X/6-31+G(d,p) level of theory is equal to 0.84 D, whereas the dipole moment of the molecule inside the C<sub>60</sub> cage becomes only slightly larger, 0.92 D (in this test the CO molecule was aligned along the *z* axis, with  $\mu_z = -0.92$  D). The dipole moment of an isolated C<sub>60</sub> molecule is zero, whereas the dipole moment of C<sub>60</sub> as part of CO@C<sub>60</sub> is 0.26 D ( $\mu_z = 0.26$  D). The dipole moment of the whole CO@C<sub>60</sub> system is 0.66 D ( $\mu_z = -0.66$  D). When an electric dipole field of 0.001 a.u. applied in any direction (*x*, *y*, or *z*), the dipole moment of CO inside CO@C<sub>60</sub> does not change, whereas the dipole moment of C<sub>60</sub> in CO@C<sub>60</sub> increases to compensate a large portion of the external field applied in that direction.

Our analysis shows that the conclusions derived in the present article about reduced and quenched polarizabilities of interior atoms are not sensitive to the choice of computational method or basis set. For example, the M06-2X/MG3 calculation of distributed polarizabilities in the neopentane molecule shows that the polarizability of the centrally situated carbon atom is nearly zero (0.04 Å<sup>3</sup>) in comparison with the total polarizability of this molecule (9.4 Å<sup>3</sup>), and the CCSD/6-31G(d) calculation also shows that the polarizability of the central carbon is ~0.04 Å<sup>3</sup> versus the total polarizability of 7.7 Å<sup>3</sup>. In addition, the conclusions derived here based on ground-state calculations can be extended to excited-state polarizabilities, and we will consider this aspect in future work.

## Acknowledgements

This work was supported in part by the U.S. Army Research Laboratory under grant no. W911NF09-100377 and by the U. S. Department of Energy, Office of Basic Energy Sciences, under SciDAC grant no. DE-SC0008666.

## Notes and references

- R. G. Parr and W. Yang, *Density-Functional Theory of Atoms and Molecules*, Oxford University Press, New York, 1989.
- J. Applequist, J. R. Carl and K.-K. Fung, *J. Am. Chem. Soc.*, 1972, **94**, 2952.
- A. J. Stone, *Mol. Phys.*, 1985, **56**, 1065.
- J. G. Angyan, G. Jansen, M. Loos, C. Hattig and B. A. Hess, *Chem. Phys. Lett.*, 1994, **219**, 267.
- F. Dehez, J.-C. Soetens, C. Chipot, J. G. Angyan and C. Millot, *J. Phys. Chem. A*, 2000, **104**, 1293.
- F. Dehez, C. Chipot, C. Millot and J. G. Angyan, *Chem. Phys. Lett.*, 2001, **338**, 180.
- M. I. H. Panhuis, P. L. A. Popelier, R. W. Munn and J. G. Angyan, *J. Chem. Phys.*, 2001, **114**, 7951.
- G. J. Williams and A. J. Stone, *J. Chem. Phys.*, 2003, **119**, 4620.
- M. I. H. Panhuis, R. W. Munn and P. L. A. Popelier, *J. Chem. Phys.*, 2004, **120**, 11479.
- L. Gagliardi, R. Lindh and G. Karlstrom, *J. Chem. Phys.*, 2004, **121**, 4494.

- 11 A. J. Misquitta and A. J. Stone, *J. Chem. Phys.*, 2006, **124**, 024111.
- 12 K. Jackson, M. Yang and J. Jellinek, *J. Phys. Chem. C*, 2007, **111**, 17952.
- 13 A. J. Misquitta, A. J. Stone and S. L. Price, *J. Chem. Theory Comput.*, 2008, **4**, 19.
- 14 F. J. Luque, F. Dehez, C. Chipot and M. Orozco, *Wiley Interdiscip. Rev.: Comput. Mol. Sci.*, 2011, **1**, 844.
- 15 D. Geldof, A. Krishtal, F. Blockhuys and C. van Alsenoy, *J. Chem. Theory Comput.*, 2011, **7**, 1328.
- 16 A. Krishtal, P. Senet, M. Yang and C. van Alsenoy, *J. Chem. Phys.*, 2006, **125**, 034312.
- 17 A. Krishtal, K. Vannomeslaeghe, D. Geldof, C. van Alsenoy and P. Geerlings, *Phys. Rev. A*, 2011, **83**, 024501.
- 18 A. Krishtal, D. Geldof, K. Vanommeslaeghe, C. van Alsenoy and P. Geerlings, *J. Chem. Theory Comput.*, 2012, **8**, 125.
- 19 P. Soderhjelm, *Theor. Chem. Acc.*, 2012, **131**, 1159.
- 20 S. W. Rick and S. J. Stuart, in *Reviews in Computational Chemistry*, ed. K. B. Lipkowitz and D. B. Boyd, Wiley-VCH, Hoboken, NJ, 2002, vol. 18, p. 89.
- 21 R. F. W. Bader, *Atoms in Molecules: A Quantum Theory*, Oxford University Press, Oxford, UK, 1990.
- 22 F. L. Hirshfeld, *Theor. Chim. Acta*, 1977, **44**, 129.
- 23 P. Bultinck, C. van Alsenoy, P. W. Ayers and R. Carbó-Dorca, *J. Chem. Phys.*, 2007, **126**, 144111.
- 24 P.-O. Löwdin, *J. Chem. Phys.*, 1950, **18**, 365.
- 25 M. J. Frisch, G. W. Trucks, H. B. Schlegel, G. E. Scuseria, M. A. Robb, J. R. Cheeseman, G. Scalmani, V. Barone, B. Mennucci, G. A. Petersson, H. Nakatsuji, M. Caricato, X. Li, H. P. Hratchian, A. F. Izmaylov, J. Bloino, G. Zheng, J. L. Sonnenberg, M. Hada, M. Ehara, K. Toyota, R. Fukuda, J. Hasegawa, M. Ishida, T. Nakajima, Y. Honda, O. Kitao, H. Nakai, T. Vreven, J. A. Montgomery Jr, J. E. Peralta, F. Ogliaro, M. Bearpark, J. J. Heyd, E. Brothers, K. N. Kudin, V. N. Staroverov, R. Kobayashi, J. Normand, K. Raghavachari, A. Rendell, J. C. Burant, S. S. Iyengar, J. Tomasi, M. Cossi, N. Rega, J. M. Millam, M. Klene, J. E. Knox, J. B. Cross, V. Bakken, C. Adamo, J. Jaramillo, R. Gomperts, R. E. Stratmann, O. Yazyev, A. J. Austin, R. Cammi, C. Pomelli, J. W. Ochterski, R. L. Martin, K. Morokuma, V. G. Zakrzewski, G. A. Voth, P. Salvador, J. J. Dannenberg, S. Dapprich, A. D. Daniels, O. Farkas, J. B. Foresman, J. V. Ortiz, J. Cioslowski and D. J. Fox, *Gaussian 09, Revision C.01*, Gaussian, Inc., Wallingford, CT, 2010.
- 26 E. J. Baerends, T. Ziegler, J. Autschbach, D. Bashford, A. Bérces, F. M. Bickelhaupt, C. Bo, P. M. Boerrigter, L. Cavallo, D. P. Chong, L. Deng, R. M. Dickson, D. E. Ellis, M. van Faassen, L. Fan, T. H. Fischer, C. Fonseca Guerra, A. Ghysels, A. Giammona, S. J. A. van Gisbergen, A. W. Götz, J. A. Groeneveld, O. V. Gritsenko, M. Grüning, S. Gusarov, F. E. Harris, P. van Den Hoek, C. R. Jacob, H. Jacobsen, L. Jensen, J. W. Kaminski, G. van Kessel, F. Kootstra, A. Kovalenko, M. V. Krykunov, E. van Lenthe, D. A. McCormack, A. Michalak, M. Mitoraj, J. Neugebauer, V. P. Nicu, L. Noodleman, V. P. Osinga, S. Patchkovskii, P. H. T. Philipsen, D. Post, C. C. Pye, W. Ravenek, J. I. Rodríguez, P. Ros, P. R. T. Schipper, G. Schreckenbach, J. S. Seldenthuis, M. Seth, J. G. Snijders, M. Solà, M. Swart, D. Swerhone, G. te Velde, P. Vernooijs, L. Versluis, L. Visscher, O. Visser, F. Wang, T. A. Wesolowski, E. M. van Wezenbeek, G. Wiesenekker, S. K. Wolff, T. K. Woo and A. L. Yakovlev, *ADF2012, SCM*, Theoretical Chemistry, Vrije Universiteit, Amsterdam, The Netherlands, 2012, <http://www.scm.com>.
- 27 A. V. Marenich, S. V. Jerome, C. J. Cramer and D. G. Truhlar, *J. Chem. Theory Comput.*, 2012, **8**, 527.
- 28 H. Yan, S. Yu, X. Wang, Y. He, W. Huang and M. Yang, *Chem. Phys. Lett.*, 2008, **456**, 223.
- 29 D. S. Sabirov and R. G. Bulgakov, *JETP Lett.*, 2011, **92**, 662.
- 30 P. Delaney and J. C. Greer, *Appl. Phys. Lett.*, 2004, **84**, 431.
- 31 T. M. Miller, in *CRC Handbook of Chemistry and Physics, 93rd ed. (2012–2013)*, ed. W. M. Haynes, CRC Press, Boca Raton, FL, 2012, pp. 10–186; <http://www.hbcpnetbase.com>, accessed 7 December 2012.
- 32 D. V. Kazachkin, Y. Nishimura, H. A. Witek, S. Irle and E. Borguet, *J. Am. Chem. Soc.*, 2011, **133**, 8191.
- 33 The Research Collaboratory for Structural Bioinformatics (RCSB), The Protein Data Bank, <http://www.rcsb.org>, accessed 9 November 2012.
- 34 J. W. Neidigh, R. M. Fesinmeyer and N. H. Andersen, *Nat. Struct. Biol.*, 2002, **9**, 425.
- 35 B. Mennucci, C. Amovilli and J. Tomasi, *Chem. Phys. Lett.*, 1998, **286**, 221.
- 36 L. Frediani, B. Mennucci and R. Cammi, *J. Phys. Chem. B*, 2004, **108**, 13796.
- 37 A. V. Marenich, C. J. Cramer and D. G. Truhlar, *J. Phys. Chem. B*, 2009, **113**, 6378.
- 38 J. J. P. Stewart, *J. Mol. Model.*, 2007, **13**, 1173.
- 39 *Maestro, version 8.5.111 and MMshare, version 1.7.110*, Schrodinger, LLC, New York, 2008.
- 40 H. W. King, in *CRC Handbook of Chemistry and Physics, 93rd ed. (2012–2013)*, ed. W. M. Haynes, CRC Press, Boca Raton, FL, 2012, pp. 12–17; <http://www.hbcpnetbase.com>, accessed 7 December 2012.
- 41 A. V. Marenich, C. J. Cramer and D. G. Truhlar, *J. Chem. Theory Comput.*, 2010, **6**, 2829.
- 42 Y. Zhao and D. G. Truhlar, *Acc. Chem. Res.*, 2008, **41**, 157.
- 43 Y. Zhao and D. G. Truhlar, *Theor. Chem. Acc.*, 2008, **120**, 215.
- 44 B. J. Lynch, Y. Zhao and D. G. Truhlar, *J. Phys. Chem. A*, 2003, **107**, 1384; see also <http://comp.chem.umn.edu/basissets/basis.cgi>, accessed 16 July 2012.
- 45 Y. Zhao and D. G. Truhlar, *J. Chem. Phys.*, 2006, **125**, 194101.
- 46 W. J. Hehre, L. Radom, P. v. R. Schleyer and J. A. Pople, *Ab Initio Molecular Orbital Theory*, Wiley, New York, 1986, p. 548.
- 47 P. L. Fast, M. L. Sanchez and D. G. Truhlar, *Chem. Phys. Lett.*, 1999, **306**, 407.
- 48 R. Krishnan, J. S. Binkley, R. Seeger and J. A. Pople, *J. Chem. Phys.*, 1980, **72**, 650.
- 49 T. Clark, J. Chandrasekhar, G. W. Spitznagel and P. v. R. Schleyer, *J. Comput. Chem.*, 1983, **4**, 294.
- 50 M. J. Frisch, J. A. Pople and J. S. Binkley, *J. Chem. Phys.*, 1984, **80**, 3265.
- 51 J. Zheng, X. Xu and D. G. Truhlar, *Theor. Chem. Acc.*, 2011, **128**, 295.